

SIMULATION OF SOFT X-RAY EMISSIVITY DURING PELLETT-INJECTION AND H-MODE IN JET

D. Pasini , A. Edwards ,R. Gill , A. Weller^(a) and D. Zasche^(a)
JET Joint Undertaking, Abingdon, Oxon., OX14 3EA, United Kingdom

^(a) *Permanent address : IPP, Garching, West Germany*

Introduction . Spatial profiles of soft X-ray intensity ($E \geq 1.75$ keV) are measured on JET using one vertical and one horizontal X-ray diode array (100 detectors total). Using tomographic reconstruction techniques spatial distributions of local X-ray emissivity are then derived. Remarkable differences in the X-ray emissivity distributions have been observed depending on the type of plasma discharge. X-ray distributions measured during limiter discharges usually have a gaussian shape. In deep contrast, extremely peaked profiles of X-ray emissivity, with most of the emission coming from a narrow central region, have been observed after pellet injection and flat or even hollow emissivity profiles have been observed during the H-mode of X-point discharges. In part 1 of this paper simulations which reproduce well both the shape and absolute emissivity of the measured profiles are presented. They show that peaked or hollow emissivity profiles reflect similar changes in the density distributions of the different species.

The vertical X-ray camera which directly views the trajectory of pellets injected into the plasma shows very intense bremsstrahlung emission from the interactions of plasma electrons with pellet particles. In part 2 of this paper a model which accounts for the main aspects of the observations will be discussed.

1. Simulation of emissivity profile .

Peaked profile – Fig. 1 shows the X-ray distribution before ($t=4.44$ s) and after ($t=7.52$ s) the injection of two D pellets (4 mm pellet at 4.5 s and 2.7 mm pellet at 5.5 s) into an ohmically heated plasma ($\#$ 13572, $I=2.5$ MA, $B=2.8$ T). The first pellet, cooling the plasma, allows the second pellet to penetrate deep into the plasma, leading to a dramatic increase of the central emissivity and consequently to a strong peaking of the X-ray distribution. Very similar observations made on other experiments have already been reported^{1,2}.

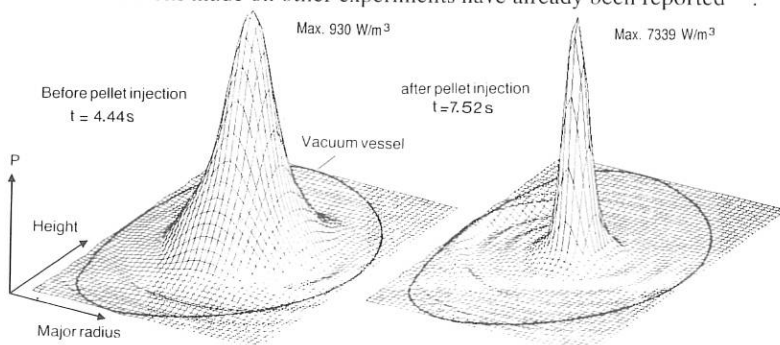


Fig. 1 – X-ray emissivity distribution before and after pellet injection.

Fig.2 shows the radial emissivity profile of the peaked distribution ($t=7.52$ s) together with two different simulations using the radiation code IONEQ³. Taking in account the transmission of the filter the code calculates for each radiating species a radial profile of emissivity and these are then summed up to yield a total profile. The radial charge state distribution for each species is calculated assuming coronal equilibrium and using the impurity concentrations derived from PHA spectra and the profiles of T_e and n_e measured with the LIDAR Thomson scattering diagnostic. The measured profile of n_e is also very peaked. In the first simulation (curve 1) which reproduces well the shape and absolute emissivity of the measured profile the density distributions of the different plasma species are assumed to be as n_e . The calculation shows that the observed emission is mainly due to free-free radiation from fully ionized C and O. In the second simulation (curve 2) the radial density distribution of D is taken as n_e but a much broader pre-pellet distribution is used for the C, O, Cl and Ni impurities. A peaked D density profile is to be expected as the second pellet deposits, in this case, a large part of its particles in the plasma center. The peaking of the impurities is more surprising and indicates an increase of the inward convection velocity. This result can be understood according to the neoclassical theory which predicts that the large density gradient of the D ions should drive the impurities inward. However since the neoclassical theory has not been adequate to describe the majority of experiments this interpretation should be looked at with caution and more work is needed to confirm it.

Hollow profile – Hollow X-ray profiles are observed in certain X-point discharges correlated with hollow electron density profiles. Fig. 3 shows such X-ray emissivity profile measured during an H-mode together with two simulations. The simulation which reproduces the measured profile well (curve 1) was obtained using the hollow electron density profile measured by interferometry and assuming for the other plasma species the same shape of density profile. A second simulation (curve 2), assuming flat density profiles over the central region, was run to verify that the hollowness in the X-ray profile was not due to line radiation from Ni or Cl but a rather a direct consequence of the hollow densities.

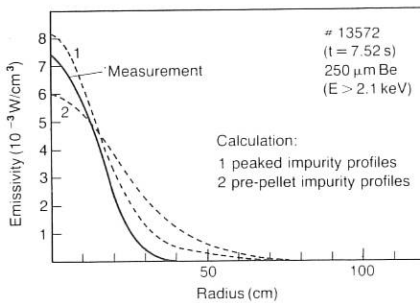


Fig. 2 – Profile of X-ray emissivity after pellet injection and two simulations assuming peaked or broad density profiles for the impurities.

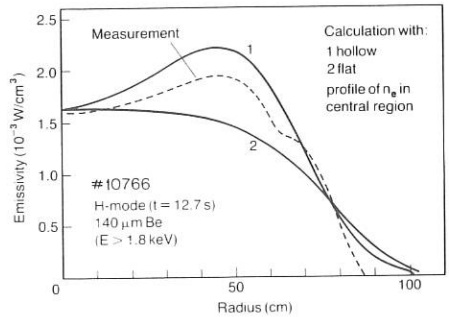


Fig. 3 – Measurement and simulation of hollow X-ray emissivity profile during an H-mode.

2. X-ray ablation emission . Detailed observations on D pellets injected into JET have been made with the vertical soft X-ray camera which directly views the pellet trajectory. Strong emission (Fig.4) is seen from the pellet-plasma interaction region due to bremsstrahlung radiation from collisions between the plasma electrons and the ablated pellet particles. The observations have been used extensively to determine the pellet velocity and depth of penetration. The time dependence of a single channel has shown that the emission originates from within a region with a diameter $2 r_c = 7 \text{ cm}$ in the major radial direction and r_c is taken as the critical radius at which the ablatant flows along the magnetic field lines. The length of the hoze of ablatant along the field lines was determined from toroidally spaced X-ray detectors as much less than 2 m . Measurements with different Be filters showed that the effective temperature of the electrons in the region of the pellet was close to that of the plasma before pellet injection.

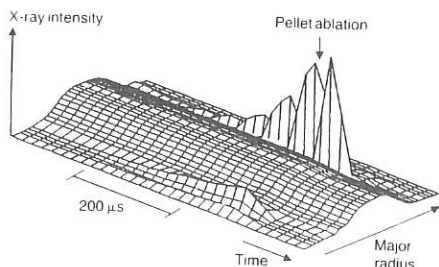


Fig. 4 - The ablation of a pellet as seen by the vertical X-ray camera.

The pellet ablation model of Parks and Turnbull⁴ has been used to calculate the absolute intensity of the X-rays. For the shots considered here the model also gave an accurate prediction of the pellet range although a more complicated model⁵ is generally required to predict the pellet range in JET. In this model the incident plasma electrons interact with the ablated particles which expand spherically with high density and low temperature near the pellet surface. In a later refinement to the theory⁶, the ablated particles flow along the magnetic field lines at $r_c = 2.5 r_p$, but we prefer to keep r_c as a free parameter as the measurements show a much larger (7x) value. Inside r_c we use the analytic asymptotic solution of PT but outside we have found the corresponding solution for cylindrical geometry. The temperature of the incident electrons differs significantly from T_e close to the pellet surface only. As the X-ray emission comes from much larger radii it is reasonable to use the plasma value of T_e everywhere. The ablatant density is

$$\rho = \rho_* \frac{1}{\alpha^{1/3}} \left(\frac{r_*}{r}\right)^{7/3}, \quad r < r_c; \quad \rho = \rho_* \frac{1}{\alpha^{1/3}} \frac{r_*^{7/3}}{r_c^2 z^{1/3}}, \quad r > r_c$$

where $\alpha^{1/3}$ is a constant near unity, r_* and ρ_* are the radius and the density at the sonic surface and z a variable along the field lines. As the velocity of the ablated particles is much less than the plasma electrons the X-ray emission may be calculated from the hydrogenic bremsstrahlung formula

$$P = 1.69 \times 10^{-32} \frac{\rho}{m} n_e \sqrt{T_e} e^{-E_c/T_e} \quad (\text{W/cm}^3)$$

where E_c is the energy cutoff. Integrating over the field of view (Fig.5) gives

$$P_x = 7.9 \times 10^{-38} \frac{\rho^*}{m} r_p^{7/3} \left\{ (D/2)^{2/3} - r_p^{2/3} \right\} n_e \sqrt{T_e} e^{-E_c/T_e} \quad (W) .$$

This expression (accurate to $\sim 20\%$) depends only weakly on r_p confirming that there is little emission from the region near to the pellet. P_x has been compared with experiment (Fig.6) for the case of a 3.6 mm D pellet injected into a D plasma with $I = 3 \text{ MA}$, $B = 2.8 \text{ T}$, $n_e = 1.35 \times 10^{19} \text{ m}^{-3}$ and $T_e = 4.8 \text{ keV}$. The calculated emission generally exceeds the observed value in the outer part of the plasma, but decreases to well below the observed value at the end of the pellet trajectory. The observation that P_x always increases sharply at the end of the trajectory is not adequately explained by this model.

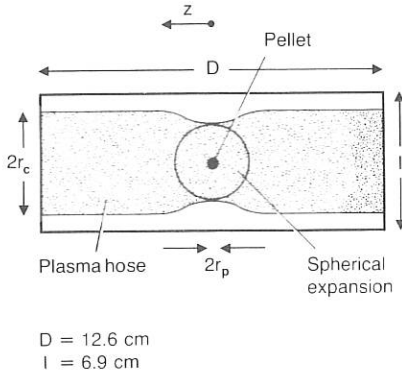


Fig. 5 - Schematic of the ablated plasma within the field of view of an X-ray detector ($D \times l$). For $r > r_c$ the particles flow along the field lines (z direction).

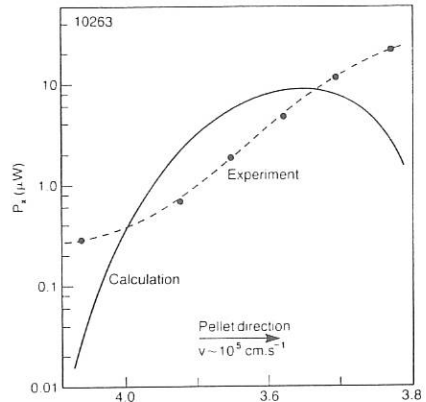


Fig. 6 - Comparison between measured (each data point corresponds to a particular detector) and calculated soft X-ray power versus radial position.

In conclusion : (1) the X-ray measurements support the concept of the formation of a plasma hose, but its radius is larger than predicted and it is quite short ($< 2m$), (2) the PT model provides an approximate estimate of the observed emission except towards the end of the pellet's range where the calculated value is much too small, (3) the X-ray energy spectrum is approximately as expected.

References

- ¹ R. Petrasco et al., Phys.Rev.Lett. 57(1986)1907.
- ² M. Greenwald et al., 11th Int. Conf. Plasma Phys. and Contr. Nucl. Fus. Res. Kyoto, 1986, IAEA-CN-47/A-III-1.
- ³ A. Weller et al. JET internal report, JET-IR(87)10. 1987.
- ⁴ P. B. Parks and R. J. Turnbull, Phys.Fluids 21(1978)1735.
- ⁵ M. L. Watkins, EPS Conf.(Schliersee) vol. 10C (1986)156.
- ⁶ P. B. Parks, Nuclear Fusion, 20(1980)311.